Spontaneous formation of dynamical patterns with fractal fronts in the cyclic lattice Lotka-Volterra model

A. Provata[1,*] and G. A. Tsekouras[1,2]
[1]*Institute of Physical Chemistry, National Research Center "Demokritos," 15310 Athens, Greece*
[2]*Department of Physics, University of Athens, 10679 Athens, Greece*
(Received 26 August 2002; published 2 May 2003)

Dynamical patterns, in the form of consecutive moving stripes or rings, are shown to develop spontaneously in the cyclic lattice Lotka-Volterra model, when realized on square lattice, at the *reaction limited* regime. Each stripe consists of different particles (species) and the borderlines between consecutive stripes are fractal. The interface width w between the different species scales as $w(L,t) \sim L^{\alpha} f(t/L^{z})$, where L is the linear size of the interface, t is the time, and α and z are the static and dynamical critical exponents, respectively. The critical exponents were computed as $\alpha = 0.49 \pm 0.03$ and $z = 1.53 \pm 0.13$ and the propagating fronts show dynamical characteristics similar to those of the Eden growth models.

DOI: 10.1103/PhysRevE.67.056602 PACS number(s): 05.40.−a, 05.10.Ln, 05.65.+b, 82.40.Np

I. INTRODUCTION

The failure of the mean-field (MF) approximation to describe processes that are restricted on low-dimensional supports has attracted considerable attention in recent years [1–10]. The presence of the support limits the efficiency of (a) the internal diffusion and (b) the external stirring (if applicable) and drives the system away from the MF expected behavior. In such cases, spatiotemporal, inhomogeneous fluctuations appear, which may introduce anomalies in the temporal evolution and/or deviations from the MF steady states [11–16]. Processes where non-MF behavior is manifested due to the presence of a support include chemical reactions on catalytic surfaces [17–26], ecology [27–29], population dynamics [30–32], and bacterial growth [33,34].

In the field of heterogeneous catalysis, in particular, model studies of reactive dynamics taking place on low-dimensional supports are most useful in the understanding of the different spatiotemporal phenomena that cannot be fully or partly explained by the MF theory. Such phenomena included fluctuations of the local concentrations, cluster formations, spatiotemporal pattern formation, nonlinear oscillations, etc., and are often observed in experiments [17–26]. A very successful model that describes the catalytic oxidation of carbon, $CO + \frac{1}{2} O_2 \rightarrow CO_2$ on the Pt catalytic surface, was introduced by Ziff, Gulari, and Barshad in 1986 [1]. This minimal model predicts kinetic phase transitions [1–6], which correspond to poisoning phenomena seen in catalytic experiments [19–21]. Similar models have also been proposed for the NO reduction on the surface of Pt [7–10]. The major success of these models is that it became possible to isolate and to identify the different mechanisms that are responsible for the various spatiotemporal phenomena observed.

In ecology and population dynamics model studies started as early as 1920 with the pioneering works of Lotka [30] and Volterra [31]. To understand the dynamics of evolution of different species Lotka and Volterra proposed MF models that predict global conservative oscillations of the species concentrations. More recently, the study of population dynamics takes into account the species distribution in space, interactions between individual species that are located in the same neighborhood, and mobility of the various species [35–37]. These studies predict the formation of spatial complex structures, phase transitions, multistability, oscillatory regions, etc.

Along these lines, and to explore complexity imposed on the dynamics due to the existence of low-dimensional supports, in a recent paper, one of the current authors (A.P.) and collaborators have introduced the (cyclic) lattice Lotka-Volterra (LLV) model [15]. The LLV model is a minimal complexity model, which can be directly implemented on lattice and involves only two reactive species X_1 and X_2 (adsorbed on a lattice support) and the empty sites of the support S. The various species are immobile on the lattice and they only react with their first neighbors. All reactive steps are bimolecular and the reactions occur via hard core interactions. Schematically, the LLV model has the following form:

$$X_1 + X_2 \xrightarrow{k_s} 2X_2, \tag{1a}$$

$$X_2 + S \xrightarrow{k_1} 2S, \tag{1b}$$

$$S + X_1 \xrightarrow{k_2} 2X_1. \tag{1c}$$

In particular, a particle X_1 adsorbed on a lattice site changes its state into X_2 when it is found in the neighborhood of another X_2 particle. Step (1a) is an autocatalytic reactive step. A particle X_2 desorbs leaving an empty site S, if in the neighborhood another empty site S is found. This step (1b) is a cooperative desorption step. Finally, a particle X_1 can be adsorbed on an empty lattice site S if in the neighborhood another X_1 particle is found. This step (1c) is a cooperative adsorption step.

*Corresponding author.
Email address: aprovata@limnos.chem.demokritos.gr

The LLV model has been studied analytically and numerically and it exhibits simple conservative oscillations at the MF level, while it demonstrates spatial concentration fluctuations and fractal pattern formation when restricted on low-dimensional supports [15].

Although in most natural processes the various species move in space via diffusion or other driving mechanisms, we explicitly ignore species mobility in the current study. This simplification is done in order to isolate the mechanisms responsible for the formation of complex structures and patterns and to examine the influence of special boundary conditions on the LLV model. Even under this simplification we show that for certain parameter values spontaneous formation of stripes is observed. Each stripe contains only particles of one type (or color) and the stripes exhibit a global average motion in the direction perpendicular to their longer axis, with a constant average velocity. Due to the dynamics of the process immobile stripes cannot be created. Since in the LLV model the reactants are considered here as immobile, they do not diffuse from one lattice site to another, the motion of the stripes is attributed to ''chemical diffusion,'' or ''color diffusion'' as will be explained in the following section, and the relative velocities depend on the reaction rates.

To understand the motion of the stripes and the formation and motion of the fractal fronts between consecutive stripes we devote one section in examining more closely the development of a fractal interface starting from a linear one (initial condition) between two different species (e.g., X_1 and X_2). This problem is here addressed from the point of view of surface growth models. We further connect the growth of fractal interfaces in the LLV model with classical surface growth models [38–40], such as the Eden model [41], the ballistic deposition model [42], the solid-on-solid models [39,43], and the curvature driven models [44–46].

In the following section we recall the main properties of the LLV model both at the MF level and by numerical simulations on a two-dimensional square lattice. In Sec. III we investigate the influence of boundary conditions on the evolution of the LLV on a square lattice. We show that for certain parameter values and under certain simple boundary conditions moving stripes are formed. In Sec. IV we examine more closely the geometry of the boundaries between adjacent stripes and rings. We show that the width of the interface grows following a scaling law, and the critical exponents describing the growth are similar to those of the Eden model. In the concluding section, we summarize our main results and discuss open problems.

II. THE LATTICE LOTKA-VOLTERRA MODEL: MEAN FIELD APPROXIMATION AND SQUARE LATTICE SIMULATIONS

The LLV model, Eqs. (1), can be described in the MF approximation via the kinetic rate equations [15]:

$$\frac{dx_1}{dt} = x_1(-k_s x_2 + k_2 s), \tag{2a}$$

$$\frac{dx_2}{dt} = x_2(k_s x_1 - k_1 s), \tag{2b}$$

$$\frac{ds}{dt} = s(-k_2 x_1 + k_1 x_2), \tag{2c}$$

where x_1, x_2, and s correspond to the mean coverage of the lattice with particles X_1, X_2, and empty sites S, respectively. In Eq. (2), the mean coverages satisfy identically the conservation condition

$$x_1 + x_2 + s = C1 = \text{const.} \tag{3}$$

It is natural for the constant to be chosen equal to 1, $C1 = 1$, corresponding to the interpretation of x_1, x_2, and s as fractions of the overall lattice, respectively, occupied by X_1 particles, X_2 particles, or being empty. Using the condition Eq. (3) with $C1 = 1$ it is possible to eliminate one of the three variables, e.g., s, from Eq. (3) and substituting into Eqs. (2) one obtains then the reduced system:

$$\frac{dx_1}{dt} = x_1[k_2 - k_2 x_1 - (k_s + k_2)x_2], \tag{4a}$$

$$\frac{dx_2}{dt} = x_2[-k_1 + (k_1 + k_s)x_1 + k_1 x_2]. \tag{4b}$$

The reduced system, Eqs. (4), admits four steady state solutions, three of which are trivial, and one nontrivial [15]:

$$x_{1s} = 0, \quad x_{2s} = 0 \quad \text{(empty lattice)}, \tag{5a}$$

$$x_{1s} = 1, \quad x_{2s} = 0 \quad \text{(lattice poisoned by } X_1\text{)}, \tag{5b}$$

$$x_{1s} = 0, \quad x_{2s} = 1 \quad \text{(lattice poisoned by } X_2\text{)}, \tag{5c}$$

$$x_{1s} = \frac{k_1}{k_1 + k_2 + k_s}, \quad x_{2s} = \frac{k_2}{k_1 + k_2 + k_s}. \tag{5d}$$

A standard linear stability analysis shows that the first three states are saddle points, while the nontrivial one is a center. Figure 1(a) depicts the phase portrait of the system for parameter values $k_1 = 0.9, k_2 = 0.3, k_s = 0.1$ and for different initial conditions. The black solid line determines the part of the phase space reserved to the system since the sum of the partial concentrations cannot exceed the value 1. The trajectories are closed curves around the center and the position of each trajectory depends solely on the initial conditions. The temporal evolution of one trajectory, corresponding to initial conditions $x_1(t=0) = 0.3$, $x_2(t=0) = 0.6$, and $s(t=0) = 0.1$, is depicted in Fig. 1(b). The motion consists of periodic, nonsymmetric oscillations and will be compared later with the corresponding Monte Carlo simulations. It can be shown that the MF system possesses a second integral of motion $C2$ [47],

$$-k_1 \ln x_1 - k_2 \ln x_2 - k_s \ln(1 - x_1 - x_2) = C2 \tag{6}$$

and thus the periodic motion extends in an infinite number of closed trajectories around the nontrivial steady state. The

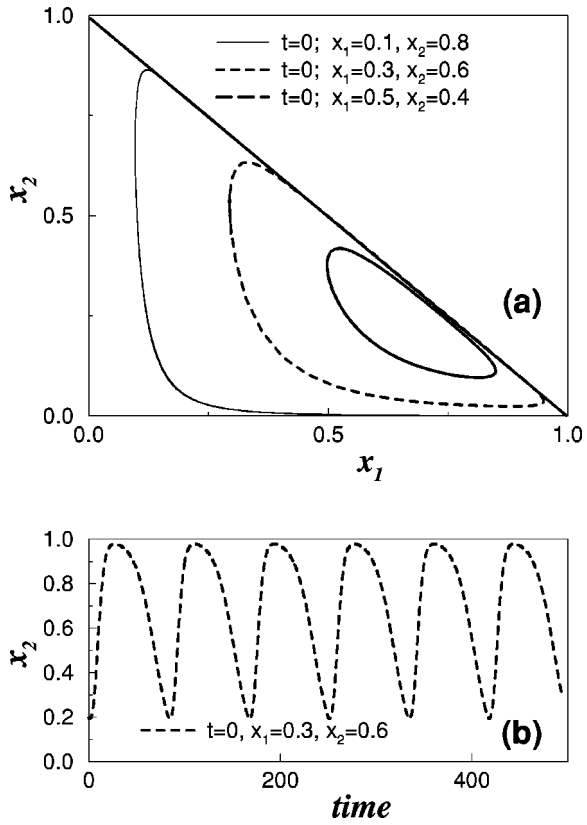

FIG. 1. (a) The phase space of the lattice Lotka-Volterra model for three different initial conditions. Parameter values are $k_1=0.9$, $k_2=0.3$, $k_s=0.1$. (b) The temporal evolution for the x_1 concentration, with the above parameters and for initial conditions $x_1(t=0)=0.3$, $x_2(t=0)=0.6$, and $s(t=0)=0.1$.

choice of the particular trajectory depends solely on the initial conditions as may be seen from Fig. 1(a).

When the system is realized on a low-dimensional surface via Monte Carlo simulations, the dimensionality of the support and, in particular, the number of nearest neighbors plays a crucial role in the outcome of the reaction. We summarize here the most important steps in the Monte Carlo realization of the LLV on the lattice, for comparison with the growth models that will be undertaken in the following section.

(1) At every microscopic step of the Monte Carlo procedure one site of the lattice is chosen at random.

(2) One of the nearest neighbors is also selected.

(3) If the original chosen site is X_1 and the selected neighbor is X_2 then the chosen site changes to X_2 with probability k_s. If the original chosen site is X_2 and the selected neighbor is S then the chosen site changes to S with probability k_1. If the original chosen site is S and the selected neighbor is X_1 then the chosen site changes to X_1 with probability k_2. Otherwise the system remains unchanged.

(4) The algorithm returns to step (1).

In the Monte Carlo procedure the unit of time is chosen as $1/N$, where N is the total number of lattice sites (occupied and empty). For example, for square lattice $N=L^2$, where L is the linear size of the lattice. With this choice of microtime, in one Monte Carlo step all lattice sites are scanned once, on the average.

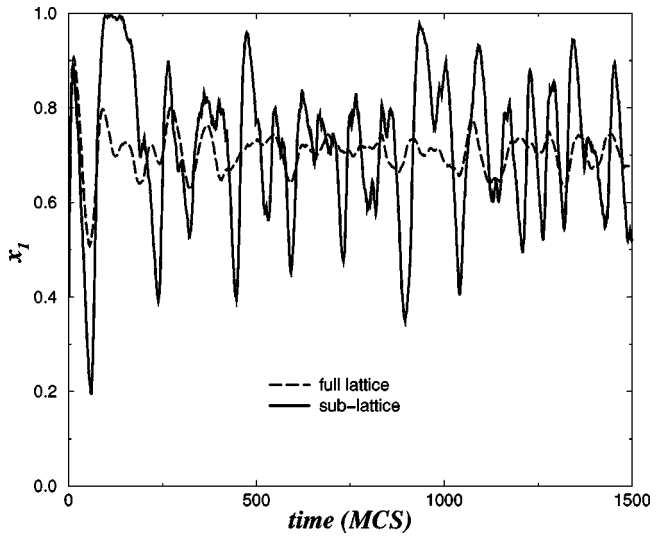

FIG. 2. Monte-Carlo simulations for the LLV model for the same parameters as in Fig. 1. The dashed line corresponds to the time evolution of the x_1 concentration over the full lattice while the solid line corresponds to the temporal evolution of the x_1 concentration on the sublattice.

For realizations on a one-dimensional lattice, it has been shown [15,16] that the system develops domains of different colors (different particles or different phases) which compete with each other and at the end only one color survives. When the system is realized on a two-dimensional square lattice substrate the system develops local domains and each domain behaves as a local oscillator with specific characteristic frequency. However, the various domains have different phases and thus, globally, no oscillation are observed, in contrast with the MF predictions [15]. In Fig. 2 the temporal evolution of the concentration of X_1 is shown as a function of time on a lattice of size $L\times L=2^8\times 2^8$ and on a sublattice of size $l\times l=2^5\times 2^5$. It is clear that while on the sublattice the concentrations show oscillatory behavior, on the entire lattice the oscillations are suppressed. Moreover, it has been shown [48] that the different species organize on local domains which present competing interactions and they have fractal boundaries. In Fig. 3 four different snapshots during the temporal evolution of the system are presented. In this figure and hereafter the X_1 particles are depicted in gray, the X_2 in white, and the empty sites in black. The initial condition was a homogeneous infinite lattice with equal concentrations of X_1,X_2 particles and empty sites S. As time increases, the system creates domains with fractal boundaries [Figs. 3(b)–3(d)]. The fractal properties of the spatial structures can be used to measure the size of the local oscillators [48]. To assure infinite lattice size in Ref. [15], periodic boundary conditions were used using a variety of lattice sizes. The role of different boundaries and inhomogeneous initial conditions will be investigated in the following section.

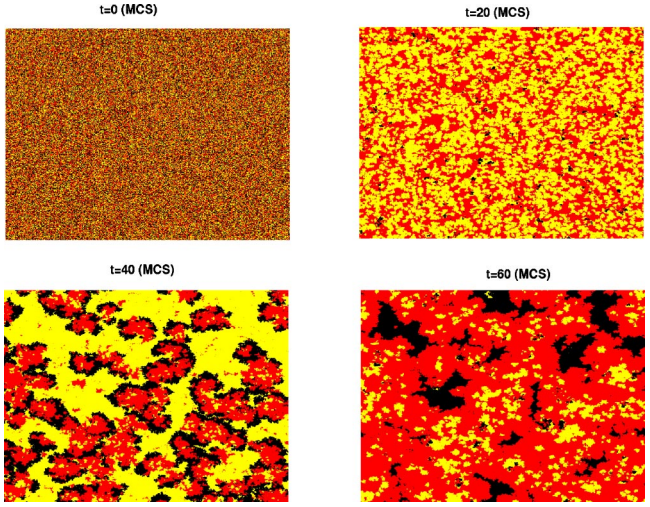

FIG. 3. Four different snapshots during the system evolution via Monte Carlo simulations. The system linear size is $L=500$ and the parameters are $k_1=0.9$, $k_2=0.3$, $k_s=0.1$.

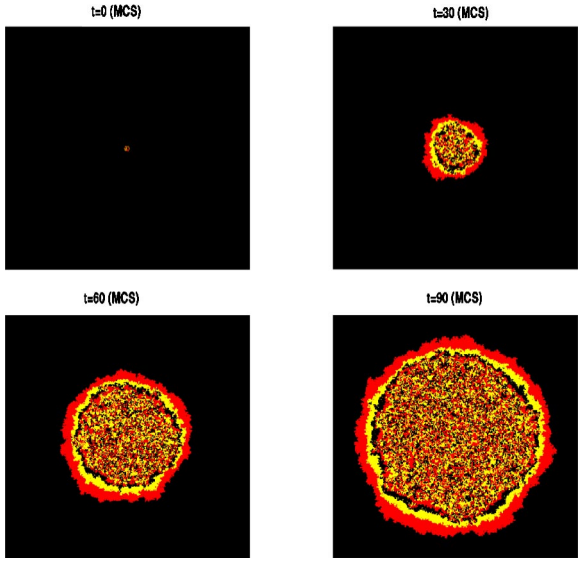

FIG. 4. (Color online) Four different snapshots during the evolution of an initially homogeneous droplet. The system linear size is $L=500$ and the parameter values are $k_1=k_2=k_s=1$.

III. THE ROLE OF INITIAL AND BOUNDARY CONDITIONS

Boundary conditions play a significant role in nonlinear dynamical system, with spatial extension. In reactive dynamics described using partial differential equations the boundary conditions may lead to the appearance of steady state spatial patterns such as dots, stripes, helices, etc. [7,49,50]. In the current study we show that the effects of various boundary conditions on the LLV model cause segregation of the complementary species near the boundary creating first a layer of specific (complementary) color. This layer induces then a second layer next to it and this way layered structures are obtained. With the term ''complementary species'' we mean species that interact with each other. In the current scheme, all three species interact with each other, however, in each interaction only one species changes its nature, while the other species plays the role of the catalyst. To be more specific, in reaction (1a) X_2 changes its nature, while X_1 plays the role of the catalyst. We say that X_2 are complements of X_1 because they tend to segregate and penetrate in regions with high density of X_1. Similarly, S are considered as complements of X_2 because they tend to concentrate and penetrate in regions with high density of X_2. Finally, X_1 are the complements of S.

In Fig. 4 the temporal evolution of an initially homogeneous droplet is presented. In the first snapshot (initial condition) a small cyclic droplet containing equal amounts of X_1 (gray), X_2 (white), and S (black), homogeneously distributed, is set in an infinite pool of empty sites S. As time increases, in the second snapshot, one layer (ring) of X_1 particles (gray) is growing in the borders of the infinite pool of S and a second ring of X_2 particles is nearly completed. The layer of X_1 particles propagates within the black, S, regions. In the third snapshot, a ring of S (complementary to X_2) appears which also propagates outwards following the X_2 rings. In the fourth snapshot another gray layer starts developing. Note that the thickness of the rings decreases with the distance from the pool. After the creation of five to six rings the thickness of the inner rings is so small that they break with the smallest fluctuation and at the center the homogeneous droplet grows. The unicolored rings move in the direction of the radius with a radial velocity that depends on the kinetic constants. In Fig. 4 all kinetic constants must have the same values, thus all the layers have the same radial velocity and consequently the patterns are statistically stable, until the outer propagating rings reach the end of the pool. If one of the kinetic constants is greater than the others then the corresponding species will prevail and will absorb all species on the outer rings.

In Fig. 5 the temporal evolution of initially homogeneous linear stripes is shown. The stripes are bordered by an infinite pool of S particles. Again, in the four snapshots the formation of linear layers, with their axis parallel to the ini-

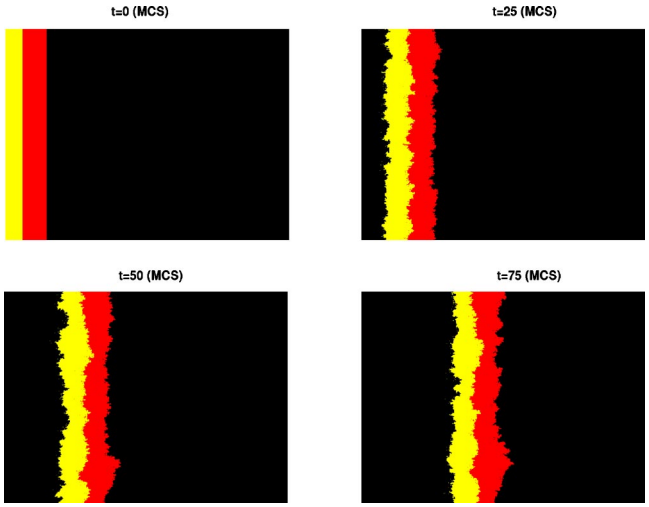

FIG. 5. Four snapshots in the development of linear diffusing fronts. Parameter values are $k_1=k_2=k_s=1$.

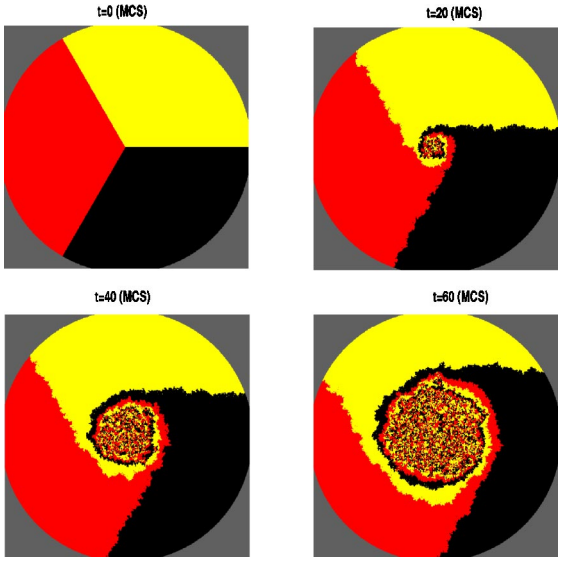

FIG. 6. (Color online) Four snapshots in the development of spiral fronts. Parameter values are $k_1=k_2=k_s=1$.

tial stripe axis are developed and all of them propagate with the same velocity. Periodic boundary conditions are taken in both x and y directions. The initially flat interfaces soon develop a rough profile that remains statistically stable, as will be calculated in Sec. IV. The kinetic constants are taken equal and thus the fronts move with the same velocity and their average thickness remains constant. The roughness of the surface depends on the linear size of the layers and the layers will break only when the value of roughness mean square deviation will reach the layer thickness.

In Fig. 6 the initial conditions are shown in the first snapshot. The three species occupy initially one third of the circle each. During evolution a spiral pattern appears propagating outwards, while in the interior a homogeneous droplet is created, surrounded by rings of different colors.

In all the above examples the existence of boundary conditions gave rise to a variety of spatiotemporal structures. These structures arise spontaneously, due (a) to the competition between the different species, (b) the boundary conditions, and (c) the lattice geometry and the boundary geometry. In the following section we simplify as much as possible (a) the interaction, keeping only two species, X_1 and X_2 and (b) the geometry, keeping only a flat initial interface between the two species. This restriction on the LLV model we call the ''two-species restricted LLV model.'' This simplification will allow to obtain quantitative results on the interface development and will contribute to the understanding of the spontaneous development of the fractal boundaries and the various spatial structures.

IV. FRONT PROPAGATION

In the case of the ''two-species restricted LLV model,'' where only particles X_1 and X_2 participate, the reaction rules are the same as in the general Monte Carlo procedure described in Sec. II, but with the absence of one species, S in the current example. Since the species S is not present in the initial state it can neither be created nor destroyed. Thus, specifically for the current example, the Monte Carlo procedure is as follows.

(1) Initially, on the square lattice, the growing surface consists of a line of size L which contains only X_2 particles. The X_1 particles represent the free space beyond the surface or interface.

(2) At every time unit, a site is chosen at random. The site can either be X_1 or X_2. If the chosen site site is X_2 then no reaction takes place and the algorithm returns to step (2).

(3) Once a particle X_1 is chosen, one of the neighbor particles is also selected at random.

(4) If the selected neighbor is X_2, the selected X_1 neighbor becomes X_2 with given constant probability (proportional to the kinetic constant). The height of the corresponding column grows then by one unit.

(5) The algorithm returns to step (2).

The propagation of the interfaces in the ''two-species restricted LLV model'' resembles very closely the surface growth of the first variation of the Eden model [41,40]. We consider Eden growth in $1+1$ dimensions. Let us call L the linear size of the substrate where the deposition takes place and $h(i,t)$ the local height of the deposit at time t. The surface growth in this variation of the Eden model takes place as follows.

(1) Initially only one line of L particles is deposited and this corresponds to the (linear) surface or interface, at $t=0$. Every particle occupies one site. Above this interface the space consists of empty cells or sites.

(2) At every time unit one surface site is randomly chosen.

(3) One of the free nearest neighbor sites is randomly selected.

(4) The selected free neighbor becomes then occupied with given constant probability and the height of the corresponding column grows by one unit.

(5) The algorithm returns to step (2).

The two models appear to be equivalent, with the only difference being that in the LLV model during each time step any particle may be selected independently of its color (X_1 or X_2) or its proximity to the interface. In contrast, in the Eden model only surface sites are chosen during the updating process. This difference results in important delays in the development of the fractal interface of the LLV model as compared with the growth of the Eden model. These delays do not alter the spatiotemporal scaling exponents in LLV, which are very close to the Eden model exponents. It should be noted that the Eden model itself shows a robustness in its scaling behavior under a variety of modifications in its growth mechanisms [38,40,41].

The same exponents are theoretically derived from the Kardar, Parisi, and Zhang (KPZ) equation in $1+1$ spatial dimensions, which involves nonlinear reactive terms and describes the growth of a variety of models with interactions between adjacent growing sites [51].

Classically the growth of interfaces is studied using the height h of the deposit and the ''interface width'' w. The average height of the deposit is defined as

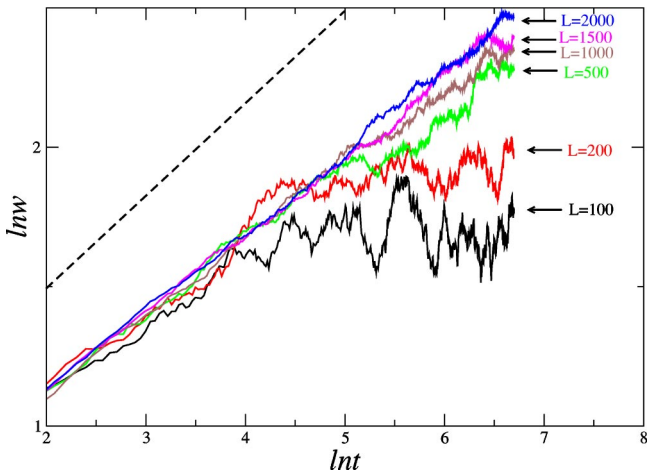

FIG. 7. The roughness w as a function of time for different values of the system size L. The parameter values are $k_1=k_2=k_s=1$.

$$\overline{h}(t)=\frac{1}{L}\sum_{i=1}^{L} h(i,t), \tag{7}$$

while the interface width w is defined as

$$w^2(L,t)=\frac{1}{L}\sum_{i=1}^{L}[h(i,t)-\overline{h}(t)]^2. \tag{8}$$

Typically, the interface width takes the form

$$w(L,t)=L^{\alpha}f\left(\frac{t}{L^z}\right), \tag{9}$$

where $f(t/L^z)$ is a scaling function that has the following form:

$$f(u)=u^{\beta} \quad \text{for} \quad u\ll 1$$
$$=\text{const} \quad \text{for} \quad u\gg 1. \tag{10}$$

Consequently, the interface width behaves with time as

$$w(L,t)\sim t^{\beta} \quad \text{for} \quad t\ll\tau$$
$$\sim L^{\alpha} \quad \text{for} \quad t\gg\tau. \tag{11}$$

The exponents β and α are called the *critical exponents*. In particular, β describes the short time behavior and is called the *growth exponent*, while α describes the steady state behavior and is called the *roughness exponent*. The system passes from short to long time behavior at the *crossover time* τ, which also depends on the system size via the *dynamic exponent* z,

$$\tau\sim L^z. \tag{12}$$

The exponents α, β, and z are not independent. It can be shown that $z=\alpha/\beta$ [40].

To determine the exponents α and β in the "two-species restricted LLV model," we have performed simulations on the two-species restricted model using lattice sizes ranging from $L=100,\ldots,2000$. The results are shown in Figs. 7 and 8. In Fig. 7 the value of the interface width w is calculated as a function of time, for various values of the linear size L. It is easy to identify a first power law growth regime followed by a saturation regime. The size of the power law regime grows with the system size and for the case of $L=2000$ (longest simulation) it extends into seven scales of magnitude. The value calculated for the exponent β is 0.32 ± 0.02. For comparison, in the same figure, the dashed line follows an exact power law with exponent $\beta_{Eden}=1/3$, which corresponds to the growth exponent of the Eden model in $1+1$ dimensions.

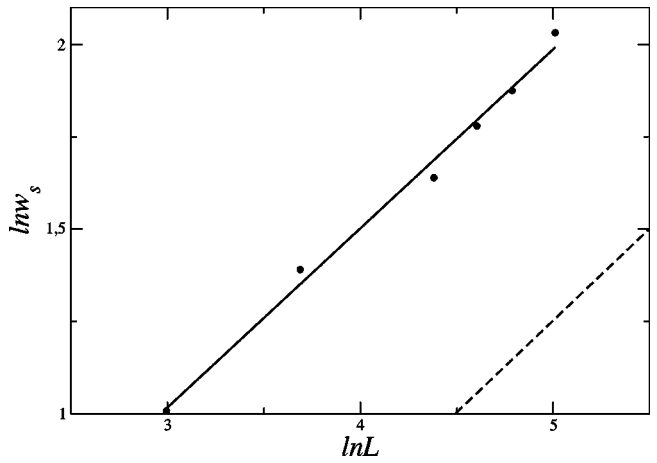

FIG. 8. The roughness w as a function of the system size L at the infinite time limit. The parameter values are $k_1=k_2=k_s=1$.

In Fig. 8 the saturation value of w is shown as a function of the system size L. The solid line is the power law fit to the data and has as exponent $\alpha=0.49\pm0.03$. For comparison, the dashed line represents an exact power law with exponent $\alpha_{Eden}=0.5$, which corresponds to the roughness exponent of the Eden model in $1+1$ dimensions. From the values of the exponents α and β the value of the dynamic exponent z is calculated as $z=1.53\pm0.13$. For comparison with the Eden model, $z_{Eden}=1.5$.

From Figs. 7 and 8 the calculation of the effective diffusion ν and effective noise correlator D in relation to the KPZ equation is possible [51–53]. These coefficients enter the $(1+1)$-dimensional KPZ equation as follows:

$$\frac{\partial h(x,t)}{\partial t}=\nu\nabla^2 h(x,t)+\frac{\lambda}{2}[\nabla h(x,t)]^2+\eta(x,t), \tag{13}$$

where $h(x,t)$ denotes the interface (or front) height at substrate position x at time t, as in Eqs. (7)–(12). $\eta(x,t)$ represents a Gaussian noise with average:

$$\langle\eta(x,t)\rangle=0 \tag{14}$$

and covariance

$$\langle\eta(x,t)\,\eta(x',t')\rangle=D\,\delta(x-x')\,\delta(t-t'). \tag{15}$$

In particular, in $(1+1)$ dimensions the KPZ equation is exactly solvable and it can be shown [52,53] that at the asymptotic limit, the interface width, as defined by Eq. (8), is

$$\langle w(L)\rangle = \left(\frac{D}{24\nu}\right)^{1/2} L^{1/2}, \quad t\to\infty, \tag{16}$$

and that

$$\langle w(t)\rangle = \frac{D}{\sqrt{2\pi\nu}} t^{\beta}, \quad t \ll \tau. \tag{17}$$

At the intermediate scaling regime, where the nonlinearity can be neglected ($\lambda=0$), the value of $\beta=1/4$, while at the onset of the nonlinear regime ($\lambda\neq 0$), $\beta=1/3$ [52]. To estimate the values of ν and D we calculate from Fig. 7 the values $w/t^{1/4}=(D/\sqrt{2\pi\nu})^{1/2}$ as a function of time. In a double logarithmic scale, at the intermediate regime, this quantity is constant in the time interval $10\,(\mathrm{MC})<t<200\,(\mathrm{MC})$ and it takes the value $(D/\sqrt{2\pi\nu})^{1/2}=1.96\pm 0.02$. Similarly the asymptotic values $w(L)/L^{1/2}=(D/24\nu)^{1/2}=0.61\pm 0.01$ are calculated from Fig. 8. Then, the effective values of the diffusion coefficient and the noise correlator are estimated as $(\nu,D)=(1.162,10.38)$. The value of ν is very important for the determination of the range of validity of the reaction limited regime when regular diffusion of particles is included in the system. In such cases if the regular diffusion constant is smaller than this effective diffusion, the reaction limited regime is justified.

From the results it is evident that the front propagation in the LLV reaction and the surface growth in the Eden model have same critical exponents. When one considers only the two-species restricted LLV model, only one reactive parameter k is relevant. The front roughness does not depend on the reactive constant, only on the rules of interaction between the neighbor particles, which are described by the Monte Carlo reactive scheme in Sec. II. The value of the reactive constant determines only the velocity of the front propagation.

The full LLV model is more complex because in each realization many fronts participate, competing with one another. The parameter values here play a key role: when the three parameters (k_1,k_2,k_s) have the same value, all fronts propagate with the same velocity, independently of the color. When the parameters have different values the different fronts propagate with different velocities depending on the colors of the interacting particles. Thus, even in a fully developed, initially random LLV system, as in Fig. 3, the borders of the different clusters have the same roughness scaling properties, even though the reactive constants k_1, k_2, and k_s are different. That is mainly the reason for the robustness of the size of the local oscillators under relatively large variations of the parameters, reported in previous works [48].

Other growth models studied in the literature, such as the ballistic deposition model [42], the solid-on-solid models [39,43], the curvature driven models [44–46], etc., present a variety of critical exponents depending on the specific growth (or deposition) rules. Alternatively, other reactive models, either involving multimolecular reactions or/and different reaction rules between neighbors are expected to produce, in general, different domain growth exponents.

V. CONCLUSIONS

In the current study the influence of initial and boundary conditions on the LLV model is studied. It is shown that starting from an initial homogeneous mixture (droplet) of X_1, X_2 and S particles, in contact with a reservoir of one of the species (e.g., S), the system spontaneously forms several unicolor layers propagating sequentially inside the reservoir. This segregation phenomenon is dynamical and cannot be observed in equilibrium. As the layers propagate through the reservoir, their size shrinks with the distance from the reservoir and when their size tends to zero the usual LLV fractal structures appear. We have seen that other boundary conditions lead to linear front propagation with surface roughening and to spiral formation and motion.

It must be stressed here that the stripe and spiral formation is due to the interaction between the different species and is not due to any particle diffusion. (Note that the reacting particles are immobile on the lattice.) One can consider the evolution as ''color diffusion'' or ''chemical diffusion'' due to interactions between neighboring particles. Also the term ''diffusion'' is not used to denote the normal Brownian motion but rather as a general term of motion of the color on the lattice.

For the simplest case of the two species restricted LLV, where fronts of one color propagate inside the complementary color, it was shown that the front propagation between the different colors has the same critical exponents with the Eden model and the KPZ equation in $1+1$ dimensions and that the roughness properties of the fronts do not depend on the parameters k_1, k_2, and k_s. This provides an explanation of the robustness of the size of the local oscillators under variations in the parameter values. From the similarity of the two-species restricted LLV model with the Eden model and the KPZ equation the effective ''color'' diffusion coefficient and noise correlator are estimated.

In the LLV model only three reactive species have been used, interacting cyclically. If more species are involved in cyclic interactions then the dynamics is further complexified and the system can present frozen patterns even in two dimensions. The geometry of the substrate also plays a very important role in the outcome of any dynamical processes. Especially in heterogeneous catalysis there might be different support geometries and phase transitions between them, reactions at terrace edges, diffusion of the various species on the support with different diffusion constants, etc. External factors, such as temperature and pressure, also influence drastically the outcome of the reactions. Further studies are needed in order to fully understand how the support properties and/or the mobility of the species modify the pattern structure and influence the steady states and the temporal evolution of dynamical systems.

[1] R.M. Ziff, E. Gulari, and Y. Barshad, Phys. Rev. Lett. **56**, 2553 (1986).
[2] B.J. Brosilow, E. Gulari, and R.M. Ziff, J. Chem. Phys. **98**, 674 (1993); C.A. Voigt and R.M. Ziff, Phys. Rev. E **56**, R6241 (1997).
[3] E.V. Albano and J. Marro, J. Chem. Phys. **113**, 10 279 (2000).
[4] P. Meakin, J. Chem. Phys. **93**, 2903 (1991).
[5] J.W. Evans and M.S. Miesch, Phys. Rev. Lett. **66**, 833 (1991); M. Tammaro and J.W. Evans, Phys. Rev. E **52**, 2310 (1995); J. Chem. Phys. **104**, 3386 (1996); **108**, 762 (1998).
[6] D.J. Liu and J.W. Evans, Phys. Rev. Lett. **84**, 955 (2000).
[7] V.P. Zhdanov, Phys. Rev. E **59**, 6292 (1999); Surf. Sci. **426**, 345 (1999); Surf. Sci. Rep. **45**, 231 (2002).
[8] H. Rose, H. Hempel, and L. Schimanksy-Geier, Physica A **206**, 421 (1994).
[9] V.P. Zhdanov, Phys. Rev. E **60**, 7554 (1995).
[10] H. Persson, P. Thormwälen, V.P. Zhdanov, and B. Kasemo, Catal. Today **53**, 273 (1999).
[11] A. Provata, J.W. Turner, and G. Nicolis, J. Stat. Phys. **70**, 1195 (1993).
[12] A. Tretyakov, A. Provata, and G. Nicolis, J. Phys. Chem. **99**, 2770 (1995).
[13] S. Prakash and G. Nicolis, J. Stat. Phys. **82**, 297 (1996).
[14] S. Prakash and G. Nicolis, J. Stat. Phys. **86**, 1289 (1997).
[15] A. Provata, G. Nicolis, and F. Baras, J. Chem. Phys. **110**, 8361 (1999).
[16] L. Frachebourg, P.L. Krapivsky, and E. Ben-Naim, Phys. Rev. E **54**, 6186 (1996).
[17] G. Ertl, Science **254**, 1750 (1991).
[18] J. Wintterlin, Adv. Catal. **45**, 131 (2000).
[19] G. Ertl, P.R. Norton, and J. Rustig, Phys. Rev. Lett. **49**, 177 (1982).
[20] M. Ehsasi, M. Matloch, O. Frank, J.H. Block, K. Christmann, F.S. Rys, and W. Hirschwald, J. Chem. Phys. **91**, 4949 (1989).
[21] R. Imbihl and G. Ertl, Chem. Rev. **95**, 697 (1995).
[22] S.Y. Shvartsman, E. Schutz, R. Imbihl, and I.G. Kevrekidis, Phys. Rev. Lett. **83**, 2857 (1999).
[23] C. Voss and N. Kruse, Ultramicroscopy **73**, 211 (1998).
[24] M. Slinko, T. Fink, T. Loher, H.H. Madden, S.J. Lombardo, R. Imbihl, and G. Ertl, Surf. Sci. **264**, 157 (1992).
[25] J. Wintterlin, S. Völkening, T.V.W. Janssens, T. Zambelli, and G. Ertl, Science **278**, 1931 (1997).
[26] N. Hartmann and R.J. Madix, Surf. Sci. **516**, 230 (2002).
[27] G. Theraulaz, E. Bonabeau, S.C. Nicolis, R.V. Sole, V. Fourcassie, S. Blanco, R. Fournier, J.L. Jolly, P. Fernandez, A. Grimal, P. Dalle, and J.L. Deneubourg, Proc. Natl. Acad. Sci. U.S.A. **99**, 9645 (2002).
[28] J.L. Deneubourg, A. Lioni, and C. Detrain, Biol. Bull. **202**, 262 (2002).
[29] F. Saffre and J.L. Deneubourg, J. Theor. Biol. **214**, 441 (2002).
[30] A.J. Lotka, Proc. Natl. Acad. Sci. U.S.A. **6**, 410 (1920).
[31] V. Volterra, *Lecons sur la Theorie Mathematique de la Lutte Pour la Vie* (Gauthier-Villars, Paris, 1931).
[32] J.D. Murray, *Mathematical Biology* (Springer, Berlin, 1993).
[33] E. Ben-Jacob, O. Shochet, A. TenenBaum, I. Cohen, A. Czirok, and T. Vicsek, Nature (London) **368**, 46 (1994).
[34] M. Matsushita and H. Fujikawa, Physica A **168**, 498 (1990).
[35] R. Monetti, A. Rozenfeld, and E. Albano, Physica A **283**, 52 (2000).
[36] T. Antal, M. Droz, A. Lipowski, and G. Odor, Phys. Rev. E **64**, 036118 (2001).
[37] M. Droz and A. Pekalski, Physica A **298**, 545 (2001).
[38] T. Vicsek, *Fractal Growth Phenomena* (World Scientific, Singapore 1989).
[39] P. Meakin, Phys. Rep. **235**, 189 (1993).
[40] A.L. Barabasi and H.E. Stanley, *Fractal Concepts in Surface Growth* (Cambridge University Press, Cambridge, 1995).
[41] M. Eden, in *Proceedings of the 4th Berkeley Symposium on Mathematical Statistics and Probability, Volume IV: Biology and Problems of Health*, edited by J. Neyman (Cambridge University Press, Berkeley, 1961).
[42] M.J. Vold, J. Phys. Chem. **63**, 1608 (1959); R. Jullien and P. Meakin, Europhys. Lett. **4**, 1385 (1987).
[43] J.M. Kim and J.M. Kosterlitz, Phys. Rev. Lett. **62**, 2289 (1989); J.G. Amar and F. Family, *ibid.* **64**, 2334 (1990).
[44] D.E. Wolf and J. Villain, Europhys. Lett. **13**, 389 (1990).
[45] S. Das Sarma and P. Tamborenea, Phys. Rev. Lett. **66**, 325 (1991).
[46] H. Park, A. Provata, and S. Redner, J. Phys. A **24**, L1391 (1991).
[47] G. Picard and T.W. Johnston, Phys. Rev. Lett. **48**, 1610 (1982).
[48] G.A. Tsekouras and A. Provata, Phys. Rev. E **65**, 016204 (2002).
[49] G. Nicolis, *Introduction to Nonlinear Science* (Cambridge University Press, Cambridge, 1995).
[50] A.S. Mikhailov, Physica A **263**, 329 (1999).
[51] M. Kardar, G. Parisi, and Y.-C. Zhang, Phys. Rev. Lett. **56**, 889 (1986).
[52] K. Sneppen, J. Krug, M.H. Jensen, C. Jayaprakash, and T. Bohr, Phys. Rev. A **46**, R7351 (1992).
[53] C.H. Lam and F.G. Shin, Phys. Rev. E **57**, 6506 (1998).